Support Vector Machines in MR Images Segmentation

[1]J. Mikulka, [2]K. Bartušek, [3]P. Dvořák

[1,3]Brno University of Technology, Brno, Czech Republic,
[2,3]Institute of Scientific Instruments ASCR, Brno, Czech Republic
Email: mikulka@feec.vutbr.cz

Abstract. *The problem most frequently encountered in the practical processing of medical images consists in the lack of instruments enabling machine evaluation of the images. A typical example of this situation is perfusion analysis of brain tumor types. The first and very significant step lies in the segmentation of individual parts of the brain tumor; after segmentation, the rate of penetration by the applied contrast agent is observed in the parts. The common method, in which a high error rate has to be considered, is to mark these tumor portions manually. The quality of brain tissue segmentation exerts significant influence on the quality of evaluation of perfusion parameters; consequently, the tumor type recognition is also influenced. The authors describe classification methods enabling the segmentation of images acquired via magnetic resonance tomography. During the edema segmentation, we obtained the following data: sensitivity 0.78±0.09, specificity 1.00±0.00, error rate 0.45±0.24 %, surface overlap 69.36±12.04 %, accuracy 99.55±0.24 %, and surface difference - 7.80±9.13 %.*

Keywords: Perfusion Analysis, Brain Tumor Segmentation, Data Classification, Support Vector Machines, Multi-parametric Segmentation.

1. Introduction

The problem of brain tissue segmentation has been widely discussed in recent years, mainly owing to the fact that the understanding of information acquired via various tomographic methods is very important for the classification of tumors, monitoring of their development, and assessment of treatment efficiency. This paper presents the development of methods for the processing of images acquired via magnetic resonance tomography (MR), a technique that finds application in various disciplines of research, for example within medicine [1], [2], agriculture, or ecology [3], [4]. The aim of the described image processing is to secure brain tumor segmentation. The area of a brain tumor can be subdivided into the actual tumor, the inner necrotic section, and the edema surrounding the tumor. An exemplary image of a tumor and its part in one slice acquired via the MR technique is provided in Fig. 1. Here, the T2-weighted image and the Turbo Spin Echo (TSE) sequence are applied to show the tumor; the slice thickness is 5 mm.All processed images were acquired in the Faculty Hospital in Brno Bohunice by the Philips Achieva MRI system (B_0 = 1.5 T).

At present, multi-parametric image analysis is frequently discussed within the scientific community [5]. This technique, even though it can be based on traditional segmentation methods (thresholding, active contours), exploits information obtained from more images or modalities at the same time. Another approach is to interpret image segmentation as the classification of multi-dimensional data. The problem of multi-parametric segmentation of MR images is described within several research reports, for example reference [6]. The authors of the report propose the segmentation of brain tissue into 15 classes; in each class, a model approximates the distribution of its parameters using Gaussian Markov random fields. For the actual segmentation, the T1, T2, Gd+T1-weighted images and perfusion images are applied.

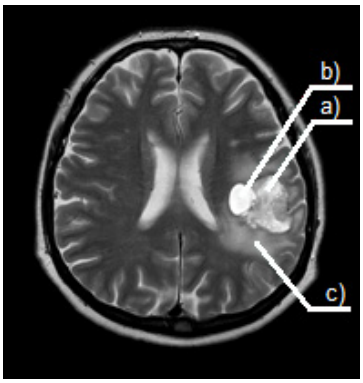

Fig. 1. Brain tumor imaging based on MR tomography; a) the tumor, b) the necrosis, c) the edema.

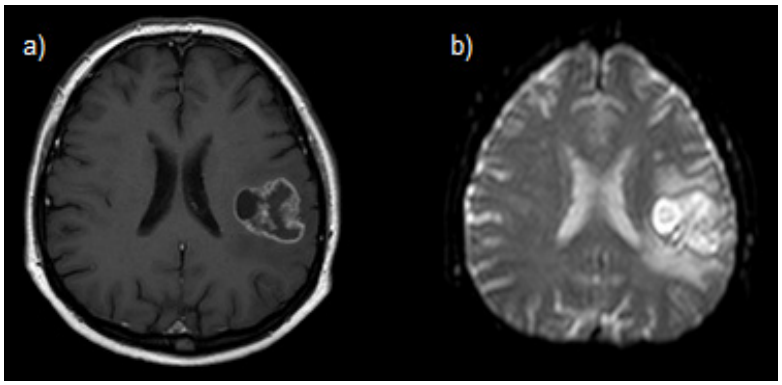

Fig. 2. a) a T1-weighted image of the tumor slice, b) a diffusion weighted image (DWI) of the tumor slice.

2. Methods for the Evaluation of Processing Quality

The proposed methods will be evaluated via calculation of the following parameters: sensitivity S_n, specificity S_p, error rate E_r, surface overlap O_S, accuracy A, and surface difference D_S. These parameters are defined as follows:

$$S_n = \frac{n_{TP}}{n_{TP} + n_{FN}}, \; S_p = \frac{n_{TN}}{n_{TN} + n_{FP}}, \qquad (1, 2)$$

$$E_r = \frac{n_{FP} + n_{FN}}{n_{TP} + n_{TN} + n_{FP} + n_{FN}} \cdot 100, \; O_S = \frac{p_S(A) \cap p_S(R)}{p_S(A) \cup p_S(R)} \cdot 100 \qquad (3, 4)$$

$$A = \frac{n_{TP} + n_{TN}}{n_{TP} + n_{TN} + n_{FP} + n_{FP}} \cdot 100, \; D_S = \frac{p_S(A) - p_S(R)}{p_S(R)} \cdot 100 \qquad (5, 6)$$

where n_{TP} is the number of true positives, n_{TN} is the number of true negatives, n_{FP} is the number of false positives, n_{FN} is the number of false negatives, $p_S(A)$ is the set of pixels inside the segmented area, and $p_S(R)$ is the set of pixels inside the ground truth area.

3. Processing of the Test Images

Description of the Proposed Method

In order to facilitate segmentation of the tumor parts, we implemented a trainable approach in the RapidMiner environment [7], [8]. The image processing chain is shown in Fig. 3.

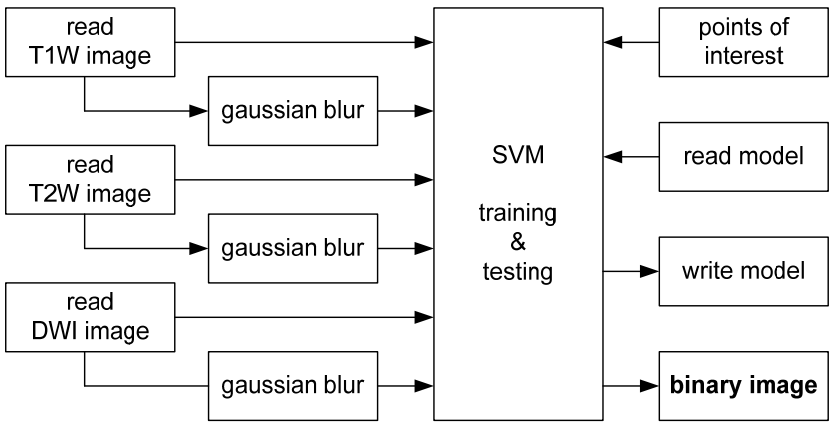

Fig. 3. The designed multi-parametric image processing chain.

The segmentation operator is realized via the Support Vector Machine (SVM) classification model with radial kernel ($\gamma = 1.0$). The aim of the classification is recognition of tumor kernel area, edema area and necrosis area in the healthy tissue. Thus, the segmentation process consists of two stages: training and testing. During the training, the pixels inside and outside the areas of interest (tumor kernel, edema and necrosis) are manually marked. The set of intensities at the marked points in the images (T1, T2, DWI) constitutes the training data of the model; then, the testing of the model is performed over the test images.

Test Image Processing Results

The segmentation results are shown in Fig. 4. The red outline indicates the brain tumor boundaries. The boundary of the surrounding edema is added to the brain tumor boundary. The areas of interest are clearly delimited by the outlines.

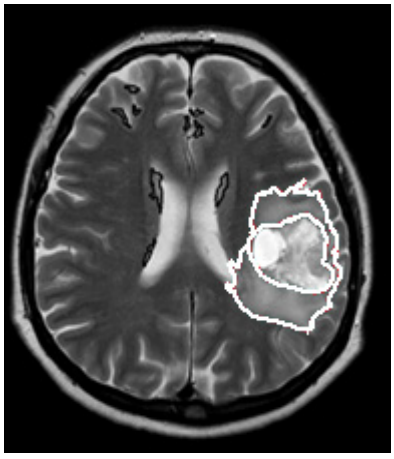

Fig. 4. Segmentation results for the tumor and edema; the ROI is marked by the white curve.

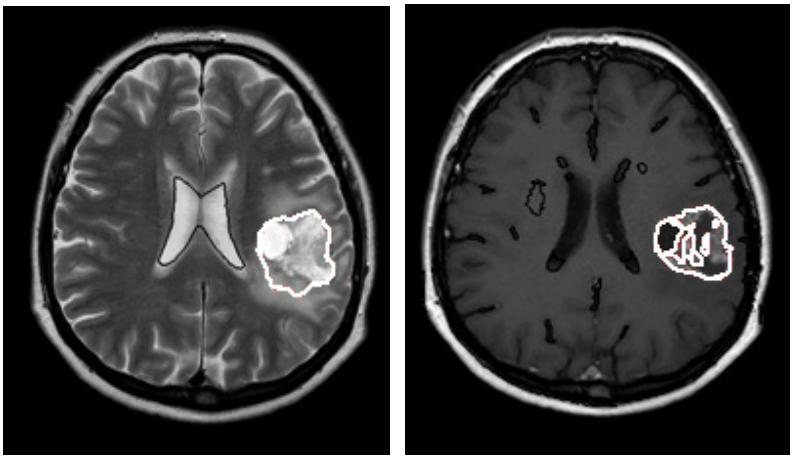

Fig. 5. Results of incorrect brain tumor segmentation realized by means of the same SVM classification method and a single input image (T2W left, T1W right).

Figure 5 shows the results of brain tumor segmentation via the SVM approach in a single image. The left section of the figure presents the results of segmentation in the T2W image, and the right section exhibits the results obtained with the T1W image. Thus, the disadvantages of single-image segmentation are clearly illustrated. In the T2W section, the outline crosses the boundaries of the edema, whose intensity is very similar to that found in the vicinity of the tumor. In the T1W image, the edema is not visible; here, segmentation fails because of inhomogeneities inside the tumor area.

Processing Quality

The processing results obtained via the designed segmentation method were compared with the ground truth segmentation approach. The results acquired in individual slices are shown in Tab. 1. The table indicates the accuracy of segmentation performed on the surrounding edema.

Table 1: Segmentation quality in the edema in several MR slices of the patient brain

Slice	S_n	S_p	E_r [%]	O_S [%]	A [%]	D_S [%]
1	0.66	1.00	0.17	58.97	99.83	-23.36
2	0.71	1.00	0.57	57.26	99.43	-4.28
3	0.87	1.00	0.41	80.92	99.59	-4.90
4	0.80	1.00	0.79	66.68	99.21	0.58
5	0.88	1.00	0.30	82.97	99.70	-7.03
mean value	0.78	1.00	0.45	69.36	99.55	-7.80

4. Conclusions

The paper presents the principles and application of classification methods for MR image segmentation. The discussed segmentation method has been designed to separate individual parts of a brain tumor, namely the actual tumor, the surrounding edema, and the necrotic tissue. The authors of this article describe a technique in which segmentation is interpreted as a set of multidimensional data. These data are then classified into pre-defined classes based on a training set. The training set is defined via manual marking of the images. Suitable metrics have been chosen to enable proper evaluation of both the similarity of the segmented area to the ground truth approach and the area location (degree of overlapping). During the edema segmentation, we obtained the following data: sensitivity $S_n = 0.78 \pm 0.09$, specificity $S_p = 1.00 \pm 0.00$, error rate $E_r = 0.45 \pm 0.24$ %, surface overlap $O_S = 69.36 \pm 12.04$ %, accuracy $A = 99.55 \pm 0.24$ %, and surface difference $D_S = -7.80 \pm 9.13$ %. These values indicate lower sensitivity of the method as well as a lower level of segment overlapping. This fact partly follows from the quality of ground truth segmentation, which always brings a certain degree of inaccuracy; this characteristic of the technique manifests itself especially in cases when the regions are not clearly delimited (the brain edema in Fig. 1c is a typical example). The error can be suppressed via extending the image training database.

Acknowledgements

This work was supported by the Grant 102/12/1104, by the project FEKT-S-11-5/1012 and by the project CZ.1.05/2.1.00/01.0017 (ED0017/01/01).

References

[1] Mikulka J, Gescheidtová E, Bartusek K. Soft-tissues Image Processing: Comparison of Traditional Segmentation Methods with 2D active Contour Methods. *Measurement Science Review*, vol. 12, pp. 153-161, ISSN 1335-8871.

[2] Bartusek K, Gescheidtova E, Mikulka J. Data processing in Studying Biological Tissues, Using MR Imaging Techniques, In 33th International Conference on Telecommunications and Signal Processing. Budapest, 2010, 171-175, ISBN 978-963-88981-0-4.

[3] Mikulka J, Gescheidtová E, Bartusek K. Perimeter Measurement of Spruce Needles Profile Using MRI. In Progress in Electromagnetics Research Symposium (PIERS 2009), Beijing, ISBN 978-1-934142-08-0.

[4] Marcon P, Bartusek K, Burdkova M. Magnetic Susceptibility Measurement Using 2D Magnetic Resonance Imaging. *Measurement Science & Technology*, 22(10), 2011, ISSN 0957-0233.

[5] Benes R, Burget R, KarásekJ, Říha K. Automatically designed machine vision system for the localization of CCA transverse section in ultrasound images. *Computer Methods and Programs in Biomedicine.* 2013, 109(3). 92-103, ISSN 0169-2607.

[6] Zavaljevski A, Dhawan A.P, Gaskil M, et al. Multi-level adaptive segmentation of multi-parameter MR brain images. *Comp. Med. Imaging and Graphics* 2000, *2*, 87-98.

[7] Burget R, Karasek J, Smekal Z, Uher V, Dostal O. Rapidminer image processing extension: A platform for collaborative research. In The 33rd International Conference on Telecommunication and Signal Processing. 2010, 114-118, ISBN 978-963-88981-0-4.

[8] Uher V, Burget R. Automatic 3D Segmentation of Human Brain Images Using Data-mining Techniques. In Proceedings of the 35th International Conference on Telecommunication and Signal Processing. 2012, 578-580, ISBN 978-1-4673-1116-8